Physical and stoichiometric controls on stream respiration in a headwater stream

Jancoba Dorley[1], Joel Singley[2,3], Tim Covino[4,5], Kamini Singha[6], Michael Gooseff[7,8], David Van Horn[9], Ricardo González-Pinzón[1]

Correspondence to: Ricardo González-Pinzón (gonzaric@unm.edu)

[1]Civil, Construction and Environmental Engineering, University of New Mexico, Albuquerque, NM USA
[2]Environmental Studies Program, University of Colorado, Boulder, CO USA
[3]Biology, Marine Biology, and Environmental Science, Roger Williams University, Bristol, RI USA
[4]Ecosystem Science and Sustainability, Colorado State University, Fort Collins, CO USA
[5]Department of Land Resources and Environmental Sciences, Montana State University, Bozeman, MT USA
[6]Geology and Geological Engineering, Hydrologic Science and Engineering Program, Colorado School of Mines, Golden, CO USA
[7]Civil, Environmental and Architectural Engineering, University of Colorado, Boulder, CO USA
[8]Institute of Arctic and Alpine Research, University of Colorado, Boulder, CO USA
[9]Department of Biology, University of New Mexico, Albuquerque, NM USA

Abstract. Many studies in ecohydrology focusing on hydrologic transport argue that longer residence times across a stream ecosystem should consistently result in higher biological uptake of carbon, nutrients, and oxygen. This consideration does not incorporate the potential for biologically mediated reactions to be limited by stoichiometric imbalances. Based on the relevance and co-dependences between hydrologic exchange, stoichiometry, and biological uptake, and acknowledging the limited amount of field studies available to determine their net effects on the retention and export of resources, we quantified how microbial respiration is controlled by the interactions and supply of essential nutrients (C, N, P) in a headwater stream in Colorado, USA. For this, we conducted two rounds of nutrient experiments, each consisting of four sets of continuous injections of Cl- as a conservative tracer, resazurin as a proxy for aerobic respiration, and one of the following nutrient treatments: a) N, b) N+C, c) N+P, and d) C+N+P. Nutrient treatments were considered as known system modifications to alter metabolism, and statistical tests helped identify the relationships between reach-scale hydrologic transport and respiration metrics. We found that as discharge changed significantly between rounds and across stoichiometric treatments, a) transient storage mainly occurred in pools lateral to the main channel and was proportional to discharge, and b) microbial respiration remained similar between rounds and across stoichiometric treatments. Our results contradict the notion that hydrologic transport alone is a dominant control on biogeochemical processing and suggest that complex interactions between hydrology, resource supply, and biological community function are responsible for driving in-stream respiration.

1 Introduction

High biochemical processing rates in streams and rivers occur at locations and times where the dynamic interconnections among hydrologic exchange, residence time, nutrient supply, and microbial biomass combine to form optimum conditions for metabolic activity (i.e., the transformation of nutrients, carbon, and oxygen or another electron acceptor into energy and biomass). The exchange of water between the main channel and transient storage zones, where most microbes exist, is the primary mechanism supplying carbon, nutrients, and oxygen to metabolically active zones (Gooseff et al. 2004; Covino et al. 2010b, 2011; Knapp et al. 2017; Gootman et al. 2020). The extent of water exchange controls the residence time of solutes (Drummond et al., 2012; Gomez et al., 2012; Patil et al., 2013), their chemical signatures (Covino and McGlynn 2007), as well as the microbial composition and their metabolic functioning (Blume et al. 2002; Navel et al. 2011; Li et al. 2020). Exchange patterns are influenced by geomorphologic conditions (Kasahara and Wondzell 2003; Cardenas et al. 2004; Gooseff et al. 2005; Emanuelson et al. 2022), hydrologic conditions (i.e., discharge and surrounding water table configuration) (Gooseff et al. 2005; Wondzell 2006; Ward et al. 2013; Ward and Packman 2019), and biofilm growth (Battin et al. 2003; Wen and Li 2018). The spatiotemporal variability in exchange processes and resource availability (e.g., seasonal variations in nutrient loads) create heterogeneous hydrologic and biogeochemical gradients across space and time, within which ecosystem metabolism occurs (Mulholland et al., 1985; Mulholland & Hill, 1997).

To date, studies with a focus on hydrologic transport argue that longer residence times across a stream ecosystem should consistently result in higher biological demand for carbon, nutrients, and oxygen (Valett et al. 1996; Gooseff et al. 2005; Wondzell 2006; Gomez et al. 2012; Zarnetske et al. 2012; Ward et al. 2013; Li et al. 2021), not fully incorporating the potential for biologically mediated reactions to be limited by stoichiometric imbalances. Ecological stoichiometry is the notion that biota balance the consumption of nutrients with energy requirements. Redfield (1934) noted that marine phytoplankton generally contained a ratio of C:N:P of 106:16:1 in their biomass, and these ratios are similar to those available in their environment. This "Redfield ratio" suggests that an ecosystem requires an optimal ratio of available nutrients to flourish and has been used as a guide for many other environmental stoichiometry studies. In a study of streams across eight biomes, Dodds et al. (2004) noted that N consumption depends in part on the C:N ratio of organic matter in streams and suggested that shifts in these state ratios likely influence N retention.

The net effect of supply and demand of resources can be explored at the reach scale with the non-dimensional Damköhler number, *Da* (Harvey et al. 2013; Pinay et al. 2015; Krause et al. 2017; Ocampo et al. 2020), which quantifies the ratio of transport (i.e., supply) to biological uptake (i.e., demand) timescales along flow paths (Oldham et al. 2013; Liu et al. 2022). Similar to any other non-dimensional number, *Da* offers simplicity and objectivity for inter-site and intra-site comparisons. *Da* has been used to provide insight into the factors limiting the supply and demand of resources (Harvey et al. 2005), as values of $Da \sim 1$ define a balance between transport and uptake time scales, which theoretically result in maximal resource retention. Accordingly, where or when $Da \ll 1$, i.e., the uptake timescale is much greater than the transport timescale, uptake is suboptimal, and it is referred to as reaction limited because even though resources became available through hydrologic exchange, they were not fully

taken up (i.e., assimilated). Conversely, where or when *Da* >>1, i.e., the transport timescale is much greater than the uptake timescale, resources become scarce or transport-limited, and biologically inactive subregions start to develop (González-Pinzón and Haggerty 2013; Harvey et al. 2013; Gootman et al. 2020). While *Da* captures essential components of the potential interactions between the supply and demand of ecologically relevant resources, it does not explicitly capture the role of stoichiometric limitations on the supply (i.e., C:N:P ratios in water fluxes) and demand (C:N:P biomass composition and needs) of resources (Tromboni et al. 2018). This is because *Da* numbers are estimated from solute-specific mass balances, which inform transport and reaction timescales for one resource at a time (e.g., only N), in isolation of other stoichiometrically relevant resources that can become limiting factors (e.g., C and P).

Based on the relevance and co-dependences between hydrologic exchange, stoichiometry, and biological uptake, and the limited amount of field studies available to determine their net effects on the retention and export of resources, we sought to quantify how metabolic activity is controlled by the interactions and supply of essential nutrients (C, N, P) at the reach scale. More specifically, we tested if variations in stoichiometric conditions can induce metabolic limitations at which residence time alone becomes a weak predictor of stream respiration. We addressed the following research question: *How is microbial respiration controlled by hydrologic exchange vs. stoichiometric conditions (i.e., supply of C, N, and P)*? We hypothesized that aerobic respiration would be maximized when nutrient supply and demand were nearly balanced for a given hydrologic condition. To test this, we conducted a repeated set of stream tracer injections in Como Creek, a mountain stream in Colorado, USA, varying stream C (acetate; sensu Baker et al., 1999), N ($NaNO_3$), and P (KH_2PO_4) concentrations to manipulate stoichiometry and nutrient supply. We repeated experiments under different flow conditions to quantify the tradeoffs between supply (transport and delivery of nutrients), and demand (microbial respiration). We tested for statistical relationships between hydrologic transport metrics and respiration metrics using the resazurin-resorufin tracer system (González-Pinzón et al., 2012; Knapp et al., 2018) and contextualized our findings within the framework of the Damköhler number.

2 Methods

2.1 Site Description

Our research experiments were conducted in Como Creek, a forested pool and riffle stream in Colorado, USA. Como Creek is a tributary to Boulder Creek, with land cover consisting of approximately 20% alpine meadow-tundra and 80% conifer forest. The study reach drains a 5.4 km^2 catchment, with elevations ranging from 2895-3557 m and a mean average precipitation of 883 mm/y (Ries III et al. 2017; Emanuelson et al. 2022). Como Creek has a snowmelt-driven hydrograph with stream discharges ranging from 1-98 L/s and features short-lived increases in discharge during the monsoon season between July and August (Figure 1). The study reach is a multi-thread channel with substrate ranging from small gravel to bedrock. Additionally, the channel has an average width-to-depth ratio of 11.5, a sinuosity of 1.1, and an average longitudinal slope of 21% (Natural Resources Conservation Service).

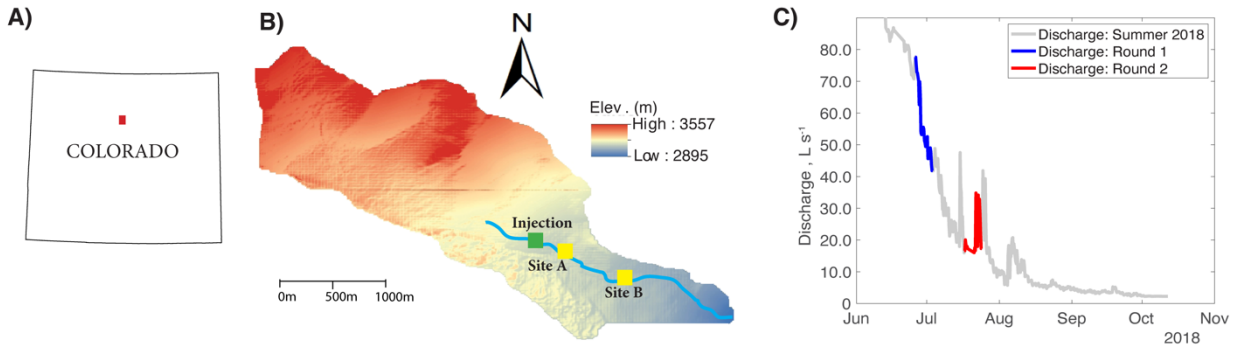

Figure 1: A) Location of Como Creek watershed in Colorado, B) detailed map of the watershed where Sites A and B are 50 and 350 m downstream from the injection location, and C) hydrograph and timing of experimental work; each round of experiments consisted of four treatments featuring N, N+C, N+P, and C+N+P nutrient additions.

2.2 Stream tracer injection experiments

We conducted two rounds of experiments, each consisting of four sets of continuous injections (lasting ~ 4-7 h) of Cl^- as a conservative tracer, resazurin (referred to as Raz hereafter) as a proxy for aerobic respiration, and one of the following nutrient treatments: a) N, b) N+C, c) N+P, and d) C+N+P. In our study, the nutrient treatments are treated as known system modifications (control variables) to alter metabolism. Also, we use the transformation of Raz, which occurred at the same spatiotemporal scales of the nutrient additions, to calculate how changes in stoichiometric conditions and discharge affect respiration. Briefly, the reactive tracer Raz (blue in color) is irreversibly reduced to resorufin (Rru, red) under aerobic respiration, and the relationship between Raz transformation and oxygen consumption is linear (González-Pinzón et al. 2012, 2014, 2016; Knapp et al. 2018; Dallan et al. 2020).

Before each tracer injection, we used the Tracer Injection Planning Tool (TIPT) (González-Pinzón et al. 2022) to estimate the amount of tracer mass needed to reach steady state conditions at the downstream site and to estimate the duration of the tracer breakthrough curves. From our field sampling, ambient concentrations of nitrate averaged 0.035 (±0.002) mg/L. We corroborated this value with a study by (Smith et al. 2003), who generated estimates of background total nitrogen (TN) and total phosphorous (TP) yield and concentrations throughout the stream-river network in 14 ecoregions of the conterminous US. That study found 75th % quartile TN= 0.21 (±0.05) mg/L and TP= 0.02 (±0.005), which indicates relatively low nutrient concentrations compared to agricultural streams in the US Midwest featuring ambient concentrations of up to two orders of magnitude higher. Based on estimated discharges and reach lengths, we targeted a maximum concentration of 2 mg/L for Cl, and 100 µg/L at the most downstream locations. The concentrations for nitrogen, phosphorus, and carbon were based on the expected detection limit of phosphate (i.e., 0.1 mg/L) for common ion chromatographs. From that minimum phosphate concentration expected, we scaled the masses of nitrogen and carbon using the 106C:16N:1P Redfield ratio (Redfield, 1934). Table 1 shows the masses injected and the discharges observed during the studies. Note that we allowed the stream to return to ambient concentrations for one day after each set of injections.

Table 1: Tracer injection data for each round of experiments at Como Creek.

Date	Treatment	Discharge (L/s)	Start time	End time	NaCl (g)	KNO_3 (g)	KPO_4 (g)	Sodium Acetate (g)	Raz (g)
Round 1									
6/26/18	N	74	11:30	17:00	32653	502	-	-	150
6/28/18	N+C	61	10:08	14:10	32680	500	-	2000	150
6/30/18	N+P	53	10:00	17:00	32680	500	400	-	150
7/2/18	C+N+P	49	9:59	14:00	32680	500	400	2000	150
Round 2									
7/17/18	N	20	10:30	14:35	10000	100	-	-	30
7/19/18	N+C	17	10:00	13:59	10000	100	-	400	30
7/21/18	N+P	17	10:00	14:06	10000	100	80	-	30
7/23/18	C+N+P	25	9:30	13:35	10000	100	80	400	30

We collected 20 mL aliquots in each tracer injection 50m and 350m downstream of the injection site (labeled Sites A and B, Figure 1) to generate tracer breakthrough curves (BTCs) for Raz. All samples were filtered immediately after being collected using a 0.7 µm GF/F filter (Sigma-Aldrich) and kept on dry ice during transport until they were frozen at -4°C for laboratory analysis for Raz concentrations. All analyses took place within a week after the end of each round of injections. At the laboratory, each sample was buffered to a pH of 8.5 (1:10 buffer-to-sample) following Knapp et al. (2018). The fluorescence signals were measured with a Cary Eclipse Fluorescence Spectrophotometer (Agilent Technologies) using excitation/emission wavelengths of 602/632 nm for Raz and 571/584 nm for Rru and converted to concentrations based on an 8-point calibration curve (R^2=0.99).

We monitored specific conductivity (SC) and temperature using Campbell Scientific CS547A sensors connected to Campbell Scientific CR 1000 dataloggers, which recorded and stored those measurements every 10 minutes. From the grab samples, we measured chloride using a Dionex ICS-1000 Ion Chromatograph with AS23/AG23 analytical and guard columns. Cl data were augmented with background-corrected SC data to model conservative transport.

We monitored changes in stream stage every 10 minutes at the end of the study reach using pressure transducers (Campbell Scientific CS420) connected to a datalogger (Campbell Scientific CR 1000). We used established stage-discharge relationships specific for the study site, as provided by the site managers. The discharge values reported in Table 1 represent mean values observed during a given experiment.

2.2 Conservative transport modelling and metrics

We calibrated the conservative transport parameters of the transient storage model presented in Equations 1 and 2 using Cl^- and streamwater electrical conductivity data observed at Sites A and B. For this, we used the Matlab (The Mathworks Inc., Natick, Massachusetts) script from Knapp et al. (2018), which features a joint calibration of conservative and reactive solutes through a non-linear, least squares optimization routine.

$$\frac{\partial c}{\partial t} = -u\frac{\partial c}{\partial x} + D\frac{\partial^2 c}{\partial x^2} - \frac{A_s}{A}\frac{\partial c_{ts}}{\partial t} + q_{in}c - \lambda_{mc}c \quad (1)$$

$$\frac{\partial c_{ts}}{\partial t} = k(c - c_{ts}) - \lambda_{ts}c_{ts} \quad (2)$$

where c [ML^{-3}] and, c_{ts} [ML^{-3}] are the concentrations in the main channel and aggregate transient storage zone; x [L] is the distance of the study reach; t [T] is time; u [LT^{-1}] and D [L^{2}T^{-1}] are parameters representing advective flow velocity and dispersion coefficient, respectively; q_{in} [T^{-1}] is a volumetric flux parameter accounting for lateral inputs; $k[T^{-1}]$ is the first-order mass transfer rate coefficient parameter between the main channel and the aggregate transient storage zone; A_s/A $[-]$ is the capacity ratio parameter representing the relative contribution of transient storage-dominated to advection-dominated compartments in the stream, represented as areas along the reach; and λ_{mc} and λ_{ts} [T^{-1}] are processing-rate coefficients in the main channel and transient storage zones (equaling zero for a conservative tracer).

We completed the parameter estimation using the Differential Evolution Adaptive Metropolis (DREAM [ZS]) algorithm (Vrugt et al. 2009). We jointly fit Cl− and Raz data in a first step of 100,000 model generations. We assessed model convergence using Gelman and Rubin $\hat{R}$ statistics (Gelman and Rubin 1992). The goodness of fit between measured and simulated BTCs was quantified through the calculation of the residual sum of squares, (nRSS) (–), normalized by the squared theoretical peak tracer concentrations of each tracer BTC of the respective tracer at the given location. The medians of the best 1,000 model simulations were used to assess the agreement between our final model fits and a subset of possible curve fits. The details on the model calibration procedure that we use in this work were presented in the supporting information of Gootman et al. (2020). Examples of observed and fitted breakthrough curves can be found in Figures S1-S3.

We estimated conservative transport timescales from the transport parameters to describe the transient storage timescale, $\tau_{sz} = 1/k$ [T], and the mean travel time between sites A and B, τ [T], which was computed as:

$$\tau = \frac{m_{1,cl}}{m_{0,cl}} \quad (3)$$

$$m_n = \sum_{i=1}^{r} \left(\frac{t_i + t_{i+1}}{2}\right)^n \left(\frac{C_i + C_{i+1}}{2}\right)(t_{i+1} - t_i) \quad (4)$$

where $m_{0,cl}$ and $m_{1,cl}$ are the zeroth and first-centralized temporal moments of the Cl$^-$ BTCs from each sampling site, i is a time index, r is the total number of samples available in a BTC.

2.3 Estimating the transformation of Raz as a proxy for microbial respiration:

We used the net transformation rate coefficients of Raz, λ_{Raz} [T^{-1}], as a proxy for microbial respiration. λ_{Raz} incorporates transformation in the main channel and in transient storage zones, and was estimated following the work by González-Pinzón and Haggerty (2013), who derived algebraic relationships with analytical solutions to calculate processing rate coefficients from the transient storage model presented in Equations 1 and 2:

$$\lambda_{Raz} = \frac{\ln\left(m_{0,Raz}^{inj}/m_{0,Raz}^{BTC}\right)}{\tau}\left(1 + \frac{\overbrace{\ln\left(m_{0,Raz}^{inj}/m_{0,Raz}^{BTC}\right)}^{dispersion\ term,\Phi}}{Pe}\right) \quad (5)$$

where $m_{0,Raz}^{inj} = M_{Raz}/Q$ is the zeroth temporal moment of Raz at the injection site [M L^{-3} T^{-1}], M_{Raz} is the mass of Raz added to the injectate, Q is the stream discharge [L^{3}T^{-1}]; $m_{0,Raz}^{BTC}$ is the dilution-corrected zeroth temporal moment of Raz estimated with BTC data from a sampling site; and $Pe = L\,u/D$ is the Peclet number [-], which

describes the relative importance of advection and dispersion in the system. As noted by González-Pinzón and Haggerty (2013), when Pe>>10, which is the case in advection-dominated systems such as open channel flow, the dispersion term Φ is negligible and $\lambda_{Raz} \approx \ln(m_{0,Raz}^{inj}/m_{0,Raz}^{BTC})/\tau$.

Since we can only get one transformation rate coefficient from every observed BTC available from Equation (5), or from the direct calibration of the transient storage model, we used the Tracer Addition for Spiraling Curve Characterization (TASCC) framework (Covino et al. 2010b) to characterize uptake kinetics over the range of experimental concentrations observed. In TASCC, the ratio of reactive to conservative solute concentrations for every independent sample across the tracer BTCs is compared to the ratio of the concentrations of the injection solution to determine uptake metrics. If the added solutes are non-reactive, they will transport conservatively, and the ratio of the reactive to conservative solute concentrations will remain constant. Alternatively, if the added solutes are limiting, co-limiting or reactive, they will not transport conservatively, and the ratio of the reactive to conservative solute concentrations will change over time as a function of reactivity. TASCC-based transformation rate coefficients for Raz were estimated using:

$$\lambda_{Raz,sample} = \frac{\ln\left[\frac{C_{Raz}}{C_{cons.}}\right]_{inj} - \ln\left[\frac{C_{Raz}}{C_{cons.}}\right]_{BTC}}{x/u}. \quad (6)$$

From each transformation rate coefficient λ_{Raz} and $\lambda_{Raz,sample}$, we also estimated an uptake (or mass transfer) velocity of Raz, $V_{f_{Raz}} = \lambda_{Raz} h$ or $V_{f_{Raz,sample}} = \lambda_{Raz,sample} h$, where h is the mean depth of the stream. Following Ensign and Doyle (2006), uptake velocities represent the vertical velocity of solute molecules through the water column towards the benthos and are typically used in stream ecology to normalize processing-rate coefficients by the influence from contrasting discharge magnitudes to facilitate the comparison of results from small streams and large rivers. As demonstrated in Covino et al. (2010b), the range of $\lambda_{Raz,sample}$ and $V_{f_{Raz,sample}}$ values encompass the λ_{Raz} and $V_{f_{Raz}}$ values obtained from processing rates derived from temporal moments analyses (e.g., Equation (5)).

Finally, reach-scale Damköhler numbers, Da [-], were calculated using the following equation:

$$Da = \frac{transient\ storage\ timescale}{transformation\ timescale} = \tau_{sz}\lambda_{Raz}. \quad (7)$$

2.4 Statistical tests

We calculated standard deviations (std) based on repeated measures of the distribution of the transport parameters of Equations 1 and 2 to create upper and lower boundaries of the uncertainties in our measurements (i.e., mean ± std). Because our data were not normally distributed, we used the Mann-Whitney U nonparametric statistical test to determine if there were statistically significant differences between nutrient treatments across rounds (e.g., N vs. N in rounds 1 and 2), following a similar procedure in Ensign and Doyle (2006). For the Mann-Whitney U test, we set our significance level (α, alpha) equal to 0.05.

We explored the Pearson correlation coefficient (r) matrix between the transport parameters of Equations 1 and 2, and associated metrics, to establish direct (r >0.1), inverse (r <-0.1), and non-existent correlations (-0.1< r <0.1) (Bowley 2008). We classified the strength of the correlations as uncorrelated (0< r <|0.1|), weakly correlated

(|0.1|< r <|0.5|), moderately correlated (|0.5|< r <|0.8|), strongly correlated (|0.8|< r <|1.0|), and included p-values for each correlation.

Lastly, we tested differences in mean values of the transport parameters of Equations 1 and 2, and associated metrics, between nutrient treatments within each experimental round (e.g., N vs. N+C vs. N+P vs. C+N+P in round 1) using the Student's *t*-test based on deviation from the group's mean value (Blair et al. 1980).

3 Results and Discussion

3.1 Conservative transport and metrics of physical controls

Between experimental rounds 1 and 2, stream depth (h) and discharge (Q) decreased, causing significant differences in stream velocity (u), dispersion (D), mass-transfer rate coefficients (k), transient storage time scales (τ_{TS}) and mean travel times (τ) (Figure 2). The only parameter that did not show significant differences was the relative contribution of the main channel to storage zone areas, A_s/A.

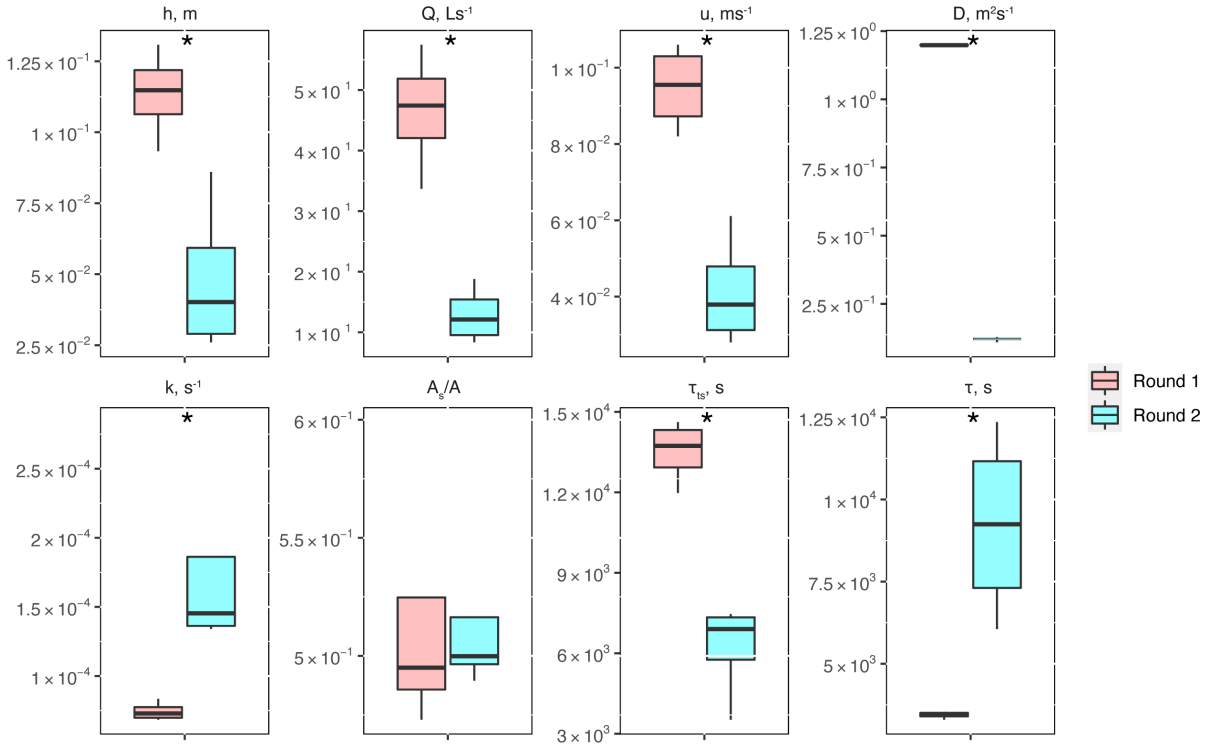

Figure 2: Conservative transport parameters and metrics of physical controls estimated for the two experimental rounds: stream depth (h), stream velocity (u), dispersion (D), mass transfer rate coefficients (k), the ratio of transient storage-dominated to advection-dominated compartments (A_s/A), transient storage time scales (τ_{TS}) and mean travel times (τ). Asterisks represent statistical differences in magnitudes for rounds 1 and 2 with p<0.05 (*) based on the Mann-Whitney U nonparametric statistical test.

The correlation matrix between parameters and metrics (Figure 3) shows that Q (and interrelated quantities h and u), D, and τ_{ts} were all directly correlated (from moderately to strongly). Mean travel times between sites, τ,

were directly and weakly correlated with k and the ratio A_s/A, and inversely correlated (from weakly to strongly) with the rest of the conservative transport parameters and metrics. Finally, the ratio A_s/A was generally uncorrelated or weakly correlated with other quantities. Even though the correlations of some interdependent quantities are known to be spurious, e.g., Q vs. u and λ_{Raz} vs. $V_{f\,Raz}$ (González-Pinzón et al. 2015), we included all relevant measured and modeled quantities in Figure 3 to allow readers to explore different data pairs. For clarity, we differentiate with brackets all known spurious correlations. Note that we did not flag the correlation between A_s/A and Q (and their interrelated quantities h and u) as spurious because the ratio of areas is an indicator of the relative volume-based contribution from advection-dominated to transient storage-dominated compartments, instead of actual estimates of cross-sectional areas (Kelleher et al. 2013; González-Pinzón et al. 2013; Knapp and Kelleher 2020).

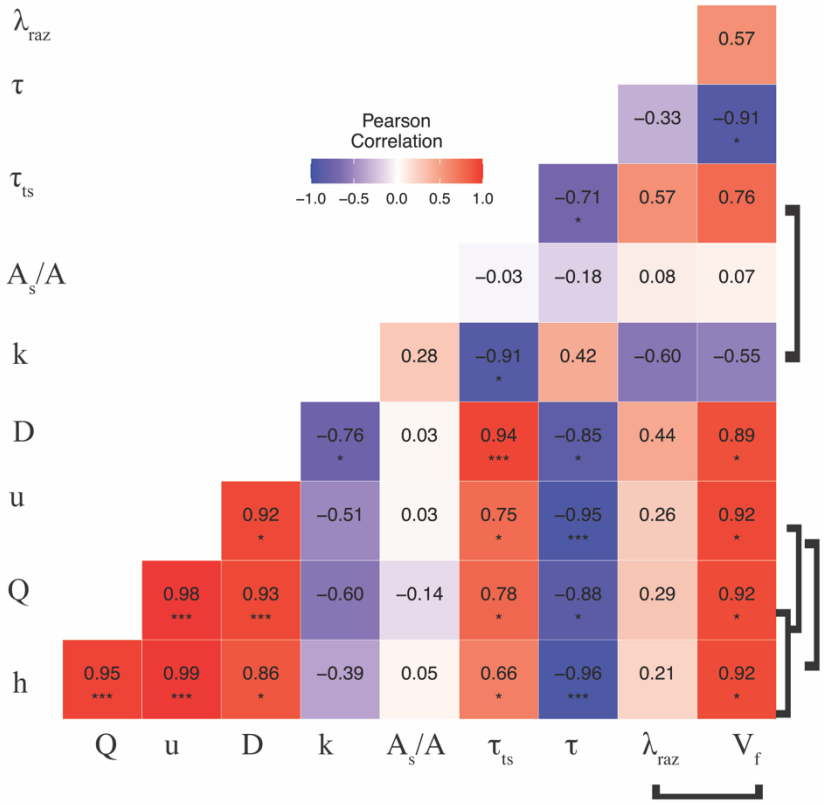

Figure 3: Pearson correlation coefficient (r) heatmap for the mean values of the transport parameters and metrics for each stoichiometric treatment during rounds 1 and 2. Brackets link known spurious correlations. Asterisks represent significant differences in magnitudes between parameters with p<0.05 (*), and p<0.001(***) based on the Pearson Correlation.

One of the metrics of interest in stream reactive-transport modeling is the transient storage timescale ($\tau_{ts} = 1/k$), which quantifies the exposure that solutes have to biological communities in metabolically active transient storage zones. In our study site, τ_{ts} decreased one order of magnitude from round 1 to round 2, and were comparable to the range of values observed in other studies involving forested mountain streams (Valett et al. 1996; Hall et al. 2002). Due to the geomorphology of the stream, which is characterized by pool and riffle sequences, but steep

longitudinal and valley slopes and shallow bedrock, transient storage was expected to occur mainly in the main channel (Fields and Dethier 2019; Barnhart et al. 2021; Emanuelson et al. 2022). As flow receded from round 1 to round 2, we observed the disconnection of in-stream pools contributing to transient storage, which explains the direct correlation between discharge and transient storage timescales. Another indication of the dominant contribution of in-stream pools to total transient storage is the lack of change of A_s/A with discharge. Since A is expected to vary proportional with discharge (i.e., $Q = A \cdot u$), a constant A_s/A suggests that the contribution of transient storage-dominated (i.e., A_s) compartments (i.e., A) also varied proportionally with discharge.

3.2 Raz transformation (a proxy for respiration) as a function of physical controls

Our results indicate that the mean values of the transformation rate coefficient of Raz (λ_{Raz}) were directly and moderately correlated with the transient storage timescale (τ_{ts}), as other studies on reactive transport have shown (Valett et al. 1996; Hall et al. 2002; Gomez et al. 2012; Zarnetske et al. 2012; Kiel and Bayani Cardenas 2014; Gootman et al. 2020). Mean λ_{Raz} values were directly and weakly correlated with discharge (Q) (also depths h and velocities u) and dispersion (D), and directly and moderately correlated with τ_{ts}. Mean λ_{Raz} values were inversely and weakly correlated with mean travel times (τ), and inversely and moderately correlated with mass-transfer rate coefficients (k) (Figure 3). Raz uptake velocities ($V_{f_{Raz}}$) showed spurious, direct and strong correlations with discharge (Q) (also h and u), strong correlations with dispersion (D) and transient storage timescales (τ_{ts}), and strong indirect correlations with mean travel times (τ) and k (moderate). Finally, both λ_{Raz} and $V_{f_{Raz}}$ were uncorrelated with A_s/A. Unlike studies where an increased transient storage timescale (τ_{ts}) is mainly associated with slower hyporheic flows due to lower discharges (Q) (Zarnetske et al. 2007; Schmid et al. 2010), τ_{ts} in our study site increased with Q because the geomorphology of the channel and the valley favored in-stream transient storage in lateral pools (Jackson et al. 2012, 2013, 2015). Similar declines in transient storage with falling discharge have been observed in other streams with comparable geomorphic characteristics (Covino et al. 2010a; Emanuelson et al. 2022), however, the absence of concurrent declines in respiration suggest biological control by some other mechanism.

3.3 Raz transformation (a proxy for respiration) as a function of physical and stoichiometric controls

Our results suggest no significant changes in respiration despite significant differences in discharge (Q), temperature, and nutrient treatments. Between experimental rounds, the mean values of Q (and h and u by extension) and temperature (except for N+C) were statistically different for each treatment comparison (Figure 4A). For $\lambda_{Raz,sample}$, we only found statistical differences between rounds for the C+N+P treatments (Figure 4C). Due to the large influence of Q on the uptake velocity of Raz ($V_{f_{Raz,sample}}$) through stream depth (h), the statistical differences between rounds seen for Q were also seen for $V_{f_{Raz,sample}}$ (Figure 4D).

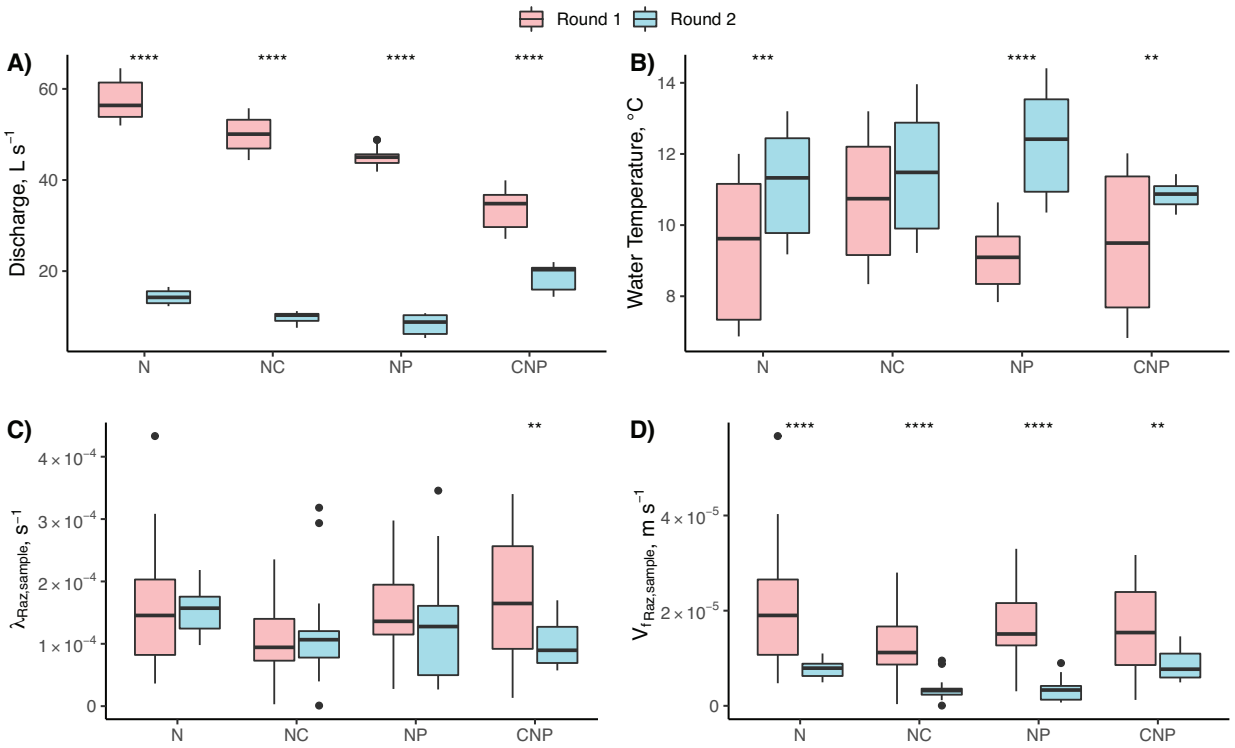

Figure 4: Comparison of A) stream discharge values recorded at the gaging station, B) stream water temperatures, C) transformation rate coefficients of resazurin ($\lambda_{Raz,sample}$) resulting from Equation 6, and associated D) uptake velocities of resazurin ($V_{f_{Raz,sample}} = \lambda_{Raz,sample}\, h$) estimated for each experimental nutrient treatment addition during rounds 1 and 2. Due to the large influence of Q on the uptake velocity of Raz ($V_{f_{Raz,sample}}$) through stream depth (h), most of the statistical differences between rounds seen for Q were also seen for $V_{f_{Raz,sample}}$. Asterisks represent significant differences in magnitudes between rounds with p<0.01(**), and p~0 (****) based on the Mann-Whitney U nonparametric statistical test.

When looking at the data collected from each round, we found that mean Q values were statistically different across nutrient treatments (Figures 5A and 5D). For mean $\lambda_{Raz,sample}$ values, the only treatments with statistical differences were the N+C and C+N+P from round 1 (Figures 5B and 5E). Finally, $V_{f_{Raz,sample}}$ mean values were only statistically different for the N vs N+C treatments for round 1, and for all but the N+C vs N+P and N vs C+N+P treatments for round 2 (Figures 5C and 5F).

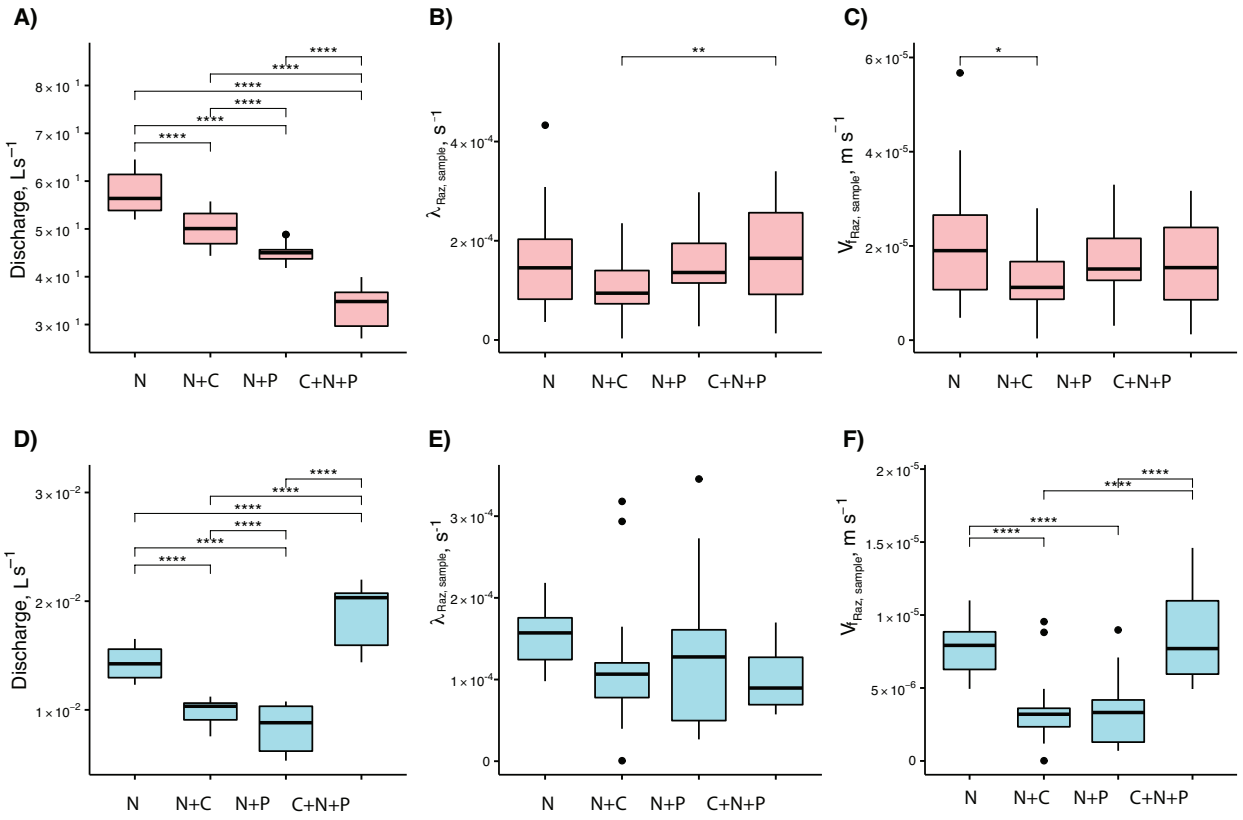

Figure 5: Comparison of stream discharges (A and D), transformation rate coefficients of resazurin ($\lambda_{Raz,sample}$) resulting from Equation 6 (B and E), and associated uptake velocities of resazurin ($V_{f_{Raz,sample}}$) (C and F) across treatments for round 1(top row) and 2 (bottom row). Due to the large influence of Q on the uptake velocity of Raz ($V_{f_{Raz,sample}}$) through stream depth (h), most of the statistical differences between rounds seen for Q were also seen for $V_{f_{Raz,sample}}$. Asterisks represent significant differences in magnitudes for treatments N, N+C, N+P, and C+N+P with p<0.05 (*), p<0.01(**), and p~0 (****) based on the Mann-Whitney U nonparametric statistical test.

For each of the eight nutrient injections, we related the mean transient storage timescales at the reach scale, τ_{ts}, which indicate exposure times between solutes and microbial communities, and the mean transformation timescales of Raz at the reach scale, $1/\lambda_{Raz}$, which indicate respiration (Figure 6). This Damköhler-based analysis allows us to visualize the interplay between physical, biological, and stoichiometric controls in the stream. We found that the range of variation of the mean transient storage timescales was three times greater than that of the mean transformation timescales. In round 1, all the stoichiometric treatments resulted in transport-limited conditions due to the high values of τ_{ts}, i.e., the average particle of Raz that entered a metabolically active compartment underwent transformation and more Raz could have been transformed if it had been available. Thus, in round 1, respiration was high relative to the supply of solutes to the metabolically active transient storage zones. In round 2, all stoichiometric treatments, except N, resulted in reaction-limited conditions, i.e., the average particle of Raz entering a metabolically active compartment left it without undergoing transformation. Thus, in round 2, respiration was slow relative to the exposure of solutes to microbial communities.

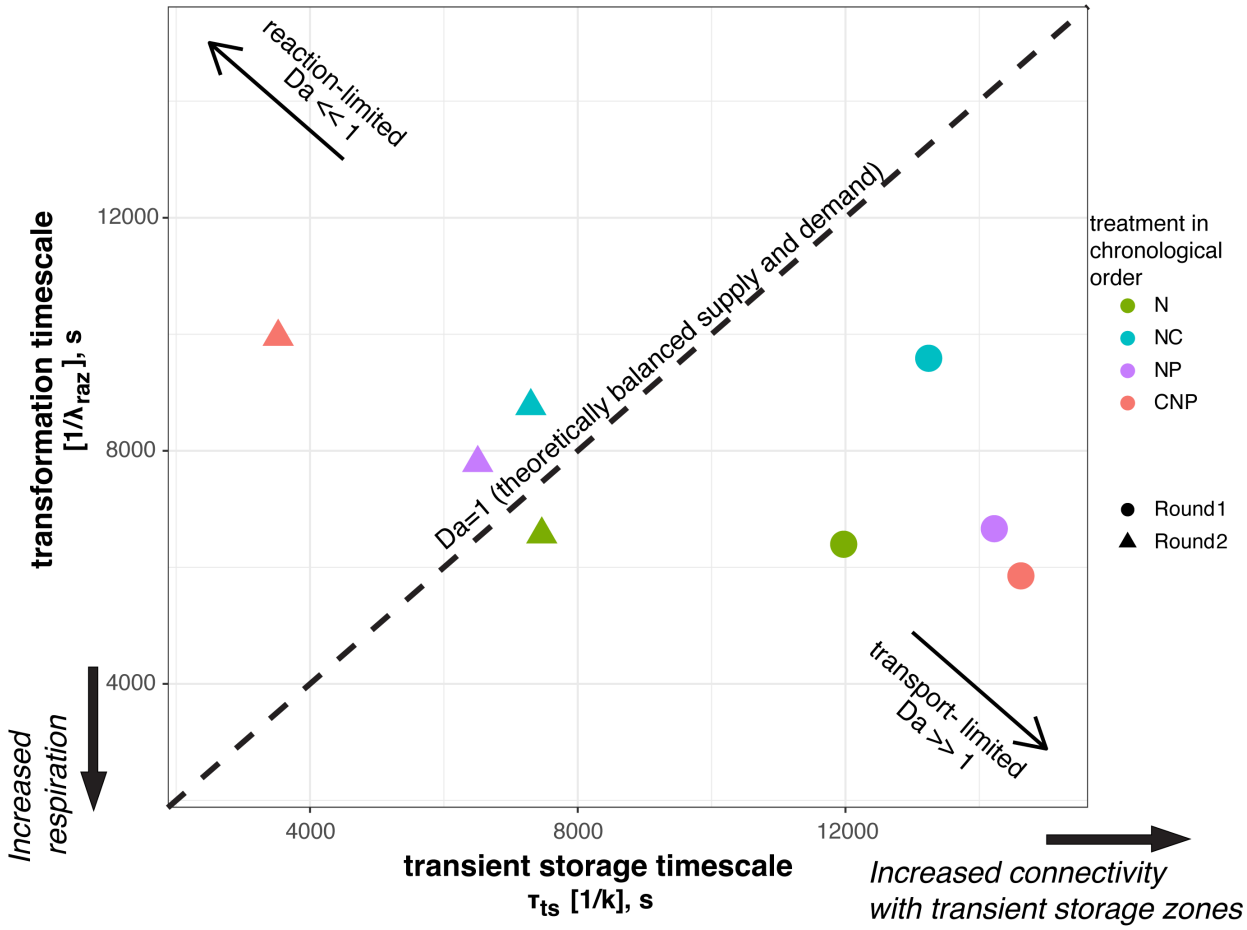

Figure 6: Mean reaction and transient storage timescales for each nutrient treatment. The Damköhler, Da = transient storage timescale/ transformation timescale, indicates reaction-limited and transport-limited conditions.

3.4 How is microbial respiration controlled by hydrologic exchange vs. stoichiometric conditions (i.e., supply of C, N, and P)?

We characterized reach-scale microbial respiration with the transformation timescale of Raz, $1/\lambda_{Raz}$; the extent of hydrologic exchanges along the reach with the transient storage timescale, τ_{TS}, and the relative size of the main channel and transient storage areas, A_s/A; and stoichiometric conditions with our controlled nutrient additions (i.e., N, N+C, N+P, and C+N+P treatments). The most salient findings indicate that a) discharge (Q) changed significantly between rounds (Figure 4a) and across stoichiometric treatments (Figure 5a, 5d), and was directly and moderately correlated with τ_{TS} and uncorrelated with A_s/A (Figure 3), suggesting that most transient storage occurred in lateral pools in the channel, which increased in quantity and extent proportionally with Q, and b) the respiration activity indicated by λ_{Raz} remained similar between rounds with significantly different Q (Figure 4b), and across controlled stoichiometric treatments also featuring different Q (Figure 5b, 5e). Thus, we observed that respiration remained largely unchanged or constant with varying physical and stoichiometric conditions.

Several hypotheses may explain the invariant reach-scale respiration observed between experimental rounds and treatments. First, tradeoffs in metabolic rates may have occurred as the stream shifted from high to low

flows. At high flows during late June and early July, lateral pools in the main channel were inundated, and transient storage timescales likely associated with these pools were high. Under these conditions, the observed respiration was probably supported by low levels of processing in the hyporheic zone due to the prevalence of bedrock substrate and relatively low respiration from benthic biomass due to scour from high flows (Francoeur and Biggs 2006; Katz et al. 2018). However, the combination of longer transient storage timescales and an expanded total surface area resulted in moderate total respiration. In contrast, during the low flows seen in the second round of injections, surface area, and transient storage timescales were decreased due to the contraction of the channel. Under these conditions, biomass increased likely due to decreased scour and increased stability (Francoeur and Biggs 2006; Katz et al. 2018; Cargill et al. 2021), increased water temperatures (Perkins et al. 2012), and increased processing of autochthonous carbon (Wagner et al. 2017) (Figure S4). This may have supported elevated areal metabolic rates in benthic biofilms (Battin et al. 2016), maintaining relatively constant respiration levels with respect to the first round of injections.

An alternative hypothesis to explain the consistency of the observed respiration values is that some other factor constraints respiration values within a narrow range. For example, the limitation of a key nutrient or metabolic resource may constrain respiration. While we designed the experiments to relieve stoichiometric constraints, it is possible that the quantities of C, N, and P in the injectate we were logistically able to introduce to the stream were insufficient to overcome demand. Also, the form of the resources may not have been readily available to communities adapted to these locals, as stream microbial communities most efficiently process the forms and diversity of dissolved organic matter found in their native habitats, and they express extracellular enzymes in ratios appropriate to acquire limiting nutrients (Hill et al. 2012; Lane et al. 2012; Wilhelm et al. 2015; Logue et al. 2016).

In previous studies, transient storage and nutrient uptake have presented contradictory relationships, which we summarize below.

Inconclusive relationships: Martí et al. (1997) did not find correlations between NH_3 uptake length and A_s/A in a desert stream using data from eight tracer injections. Webster et al. (2003) did not find statistically significant relationships between NH_4 uptake and A_s/A using the 11-stream LINX-I dataset that included arctic to tropical streams. From thirty seven injections conducted in thirteen streams at Hubbard Brook Experimental Forest (HBEF), Hall et al. (2002) found weak correlations (R^2=0.14-0.35) between transient storage parameters and NH_4 demand. Using data from seven streams in New Zealand, Niyogi et al. (2004) did not find significant correlations between soluble reactive phosphorous (P-SRP), NO_3 uptake velocities, and A_s/A. Bukaveckas (2007) reported an indefinite relationship between transient storage and NO_3 and P-SRP retention efficiencies from tracer injections in a reference (N=13 injections), a channelized (N=14 injections), and a restored (N=17 injections) stream reach in the midwestern US. Lastly, the LINX-II dataset from ^{15}N-NO_3 injections in 72 streams located in eight regions of the US showed no relationship between NO_3 uptake and the fraction of median travel time due to transient storage (F_{med}^{200}) (Hall et al. 2009).

Weak to moderate relationships: Thomas et al. (2003) showed that transient storage accounted for 44% to 49% of NO_3 retention measured by ^{15}N in a small headwater stream in North Carolina. Mulholland et al. (1997) found larger PO_4 uptake rates in a stream with higher transient storage, when they compared two forested streams. Ensign and Doyle (2005) found an increase in A_s/A and the uptake velocities for NH_4 and PO_4 after the addition of

flow baffles to two streams. Lautz and Siegel (2007) found a modest correlation (R^2=0.44) between NO_3 retention efficiency and transient storage in the Red Canyon Creek watershed, WY.

Strong relationships: Valett et al. (1996) found a strong correlation (R^2=0.77) between transient storage and NO_3 retention in three first-order streams in New Mexico. From nine tracer injections in two urban streams in the eastern US, Ryan et al. (2007) found strong relationships between P-SRP retention and transient storage metrics ($k, A_s/A$; R^2>0.84) when the variables were measured in different seasons. Sheibley et al. (2014) observed that the retention of NO_3 in seven agricultural streams in the US was positively correlated with A_s/A and the average water flux through the storage zone per unit length of stream ($q_s = kA$), and negatively correlated with the transient storage timescale (τ_{ts}). However, they found no significant correlation between NH_4^+ and SRP retention and transient storage metrics.

The studies referenced above were performed in streams with contrasting physical, chemical, and biological conditions. Together, they offer a broader perspective on the inconsistent relationship between transient storage metrics and metabolic processing. Those studies do not feature co-injections of C, N, and P macronutrients (e.g., N+C, N+P, N+C+P), even while some tracked ambient processing rates of more than one nutrient. Therefore, they generally represent solute-specific analyses, where the uptake of one nutrient at a time was analyzed and, thus, did not account for stoichiometric controls on nutrient uptake (however, see Tromboni et al. (2018) for an example of recent trend changes in this research area). By combining both transport and stoichiometric analyses, our study offers evidence that stoichiometric controls have an ambiguous relationship to reach-scale metabolic activities, and that further investigations should be conducted using greater quantities and types of resources.

4 Conclusions

We conducted two rounds of four stoichiometric treatments (i.e., N, C+N, N+P, and C+N+P) in a headwater stream in Colorado to quantify reach-scale changes to stream respiration during flow recession and answer the question: *How is respiration controlled by hydrologic exchange vs. stoichiometric conditions (i.e., supply of C, N, and P)*? We found that discharge changed significantly between rounds and across stoichiometric treatments, and that it was directly and moderately correlated with transient storage timescales but uncorrelated with the ratio of contributions from advection-dominated to transient storage-dominated compartments (i.e., A_S/A). This suggests that most transient storage occurred in lateral pools within the main channel, which increased in quantity and extent proportionally with discharge. We also found that respiration remained similar despite significant changes in discharge and stoichiometric treatments. Our results contradict the notion that hydrologic transport alone is a dominant control on biogeochemical processing, and suggest that complex interactions between hydrology, resource supply, and biological community function are responsible for driving in-stream respiration.

Author contribution: RGP, TC, KS, and MG secured the funding for this research. All co-authors designed carried out the experiments. JD and RGP processed Raz samples, performed solute transport simulations, statistical analyses,

and prepared the manuscript with input from all co-authors. DVH supported the contextualization of hydrological and ecological interactions. All co-authors approved the final version of the manuscript.

Competing interests: The authors declare no competing interests.

Acknowledgments

The National Science Foundation provided funding support through grants NSF EAR-1642399, NSF EAR-1642368, NSF EAR-1642402, NSF EAR-1642403, and NSF 1914490. We thank Karin Emanuelson, Jackie Randell, Erin Jenkins, Tristan Weiss, and Melissa Pinzon for their field and laboratory assistance.

Data availability: The data used in his article can be found in the CUAHSI HydroShare repository. Gonzalez-Pinzon, R. (2022). Resazurin tracer data from experiments in Colorado (2018) and Iowa (2019), HydroShare, http://www.hydroshare.org/resource/50ae3c59bebe4cb383e31408a0c10012

References

Barnhart, T. B., J. Vukomanovic, P. Bourgeron, and N. P. Molotch. 2021. Future land cover and climate may drive decreases in snow wind-scour and transpiration, increasing streamflow at a Colorado, USA headwater catchment. Hydrol. Process. **35**: e14416. doi:10.1002/hyp.14416

Battin, T. J., K. Besemer, M. M. Bengtsson, A. M. Romani, and A. I. Packmann. 2016. The ecology and biogeochemistry of stream biofilms. Nat. Rev. Microbiol. **14**: 251–263. doi:10.1038/nrmicro.2016.15

Battin, T. J., L. A. Kaplan, J. D. Newbold, and C. M. E. Hansen. 2003. Contributions of microbial biofilms to ecosystem processes in stream mesocosms. Nature **426**: 439–442. doi:10.1038/nature02152

Blair, R. C., J. J. Higgins, S. Journal, and N. Winter. 1980. A Comparison of the Power of Wilcoxon ' s Rank-Sum Statistic to That of Student ' s t Statistic under Various Nonnormal Distributions Published by : American Educational Research Association and American Statistical Association Stable URL : https://www.jstor.org/stable/1164905 REFERENCES Linked references are available on JSTOR for this article : reference # references _ tab _ contents You may need to log in to JSTOR to access the linked references . **5**: 309–335.

Blume, E., M. Bischoff, J. M. Reichert, T. Moorman, A. Konopka, and R. F. Turco. 2002. Surface and subsurface microbial biomass, community structure and metabolic activity as a function of soil depth and season. Appl. Soil Ecol. **20**: 171–181. doi:10.1016/S0929-1393(02)00025-2

Bowley, A. L. 2008. The Standard Deviation of the Correlation Coefficient Author (s): A . L . Bowley Source : Journal of the American Statistical Association , Vol . 23 , No . 161 (Mar ., 1928), pp . 31- Published by : American Statistical Association Stable URL : http:/. J. Am. Stat. Assoc. **23**: 31–34.

Bukaveckas, P. A. 2007. Effects of Channel Restoration on Water Velocity, Transient Storage, and Nutrient Uptake in a Channelized Stream. Environ. Sci. Technol. **41**: 1570–1576. doi:10.1021/es061618x

Cardenas, M. B., J. L. Wilson, and V. A. Zlotnik. 2004. Impact of heterogeneity, bed forms, and stream curvature on subchannel hyporheic exchange. Water Resour. Res. **40**: 1–14. doi:10.1029/2004WR003008

Cargill, S. K., C. Segura, S. R. Villamizar, and D. R. Warren. 2021. The influence of lithology on stream metabolism in headwater systems. Ecohydrology **14**. doi:10.1002/eco.2284

Covino, T. P., B. McGlynn, and M. Baker. 2010a. Separating physical and biological nutrient retention and quantifying uptake kinetics from ambient to saturation in successive mountain stream reaches. J. Geophys. Res. Biogeosciences **115**: 1–17. doi:10.1029/2009JG001263

Covino, T. P., and B. L. McGlynn. 2007. Stream gains and losses across a mountain-to-valley transition: Impacts on watershed hydrology and stream water chemistry. Water Resour. Res. **43**: 1–14. doi:10.1029/2006WR005544

Covino, T. P., B. L. Mcglynn, and R. A. Mcnamara. 2010b. Tracer Additions for Spiraling Curve Characterization (TASCC): Quantifying stream nutrient uptake kinetics from ambient to saturation. Limnol. Oceanogr. Methods 484–498. doi:10.4319/lom.2010.8.484

Covino, T. P., B. McGlynn, and J. Mallard. 2011. Stream-groundwater exchange and hydrologic turnover at the network scale. Water Resour. Res. **47**: 1–11. doi:10.1029/2011WR010942

493 Dallan, E., P. Regier, A. Marion, and R. González-Pinzón. 2020. Does the Mass Balance of the
494 Reactive Tracers Resazurin and Resorufin Close at the Microbial Scale? J. Geophys. Res.
495 Biogeosciences **125**: 1–10. doi:10.1029/2019JG005435
496 Emanuelson, K., T. P. Covino, A. S. Ward, J. Dorley, and M. N. Gooseff. 2022. Conservative
497 solute transport processes and associated transient storage mechanisms: Comparing
498 streams with contrasting channel morphologies, land use and land cover. Hydrol. Process.
499 **36**.
500 Ensign, S. H., and M. W. Doyle. 2005. In-channel transient storage and associated nutrient
501 retention: Evidence from experimental manipulations. Limnol. Oceanogr. **50**: 1740–1751.
502 doi:10.4319/lo.2005.50.6.1740
503 Ensign, S. H., and M. W. Doyle. 2006. Nutrient spiraling in streams and river networks. J.
504 Geophys. Res. Biogeosciences **111**. doi:10.1029/2005jg000114
505 Fields, J. F., and D. P. Dethier. 2019. From on high: Geochemistry of alpine springs, Niwot
506 Ridge, Colorado Front Range, USA. Hydrol. Process. **33**: 1756–1774.
507 doi:10.1002/hyp.13436
508 Francoeur, S. N., and B. J. F. Biggs. 2006. Short-term Effects of Elevated Velocity and Sediment
509 Abrasion on Benthic Algal Communities. Hydrobiologia **561**: 59–69.
510 doi:10.1007/s10750-005-1604-4
511 Gelman, A., and D. B. Rubin. 1992. Inference from Iterative Simulation Using Multiple
512 Sequences. Stat. Sci. **7**. doi:10.1214/ss/1177011136
513 Gomez, J. D., J. L. Wilson, and M. B. Cardenas. 2012. Residence time distributions in sinuosity-
514 driven hyporheic zones and their biogeochemical effects. Water Resour. Res. **48**: 1–17.
515 doi:10.1029/2012WR012180
516 González-Pinzón, R., J. Dorley, J. Singley, K. Singha, M. Gooseff, and T. Covino. 2022. TIPT:
517 The Tracer Injection Planning Tool. Environ. Model. Softw. **156**: 105504.
518 doi:10.1016/j.envsoft.2022.105504
519 González-Pinzón, R., and R. Haggerty. 2013. An efficient method to estimate processing rates in
520 streams. Water Resour. Res. **49**: 6096–6099. doi:10.1002/wrcr.20446
521 González-Pinzón, R., R. Haggerty, and A. Argerich. 2014. Quantifying spatial differences in
522 metabolism in headwater streams. Freshw. Sci. **33**: 798–811. doi:10.1086/677555
523 González-Pinzón, R., R. Haggerty, and M. Dentz. 2013. Scaling and predicting solute transport
524 processes in streams. Water Resour. Res. **49**: 4071–4088. doi:10.1002/wrcr.20280
525 González-Pinzón, R., R. Haggerty, and D. D. Myrold. 2012. Measuring aerobic respiration in
526 stream ecosystems using the resazurin-resorufin system. J. Geophys. Res. Biogeosciences
527 **117**: 1–10. doi:10.1029/2012JG001965
528 González-Pinzón, R., J. Mortensen, and D. Van Horn. 2015. Comment on "Solute-specific
529 scaling of inorganic nitrogen and phosphorus uptake in streams" by Hall et al. (2013).
530 Biogeosciences **12**: 5365–5369. doi:10.5194/bg-12-5365-2015
531 González-Pinzón, R., M. Peipoch, R. Haggerty, E. Martí, and J. H. Fleckenstein. 2016.
532 Nighttime and daytime respiration in a headwater stream. Ecohydrology **9**: 93–100.
533 doi:10.1002/eco.1615
534 Gooseff, M. N., K. E. Bencala, D. T. Scott, R. L. Runkel, and D. M. McKnight. 2005. Sensitivity
535 analysis of conservative and reactive stream transient storage models applied to field data
536 from multiple-reach experiments. Adv. Water Resour. **28**: 479–492.
537 doi:10.1016/j.advwatres.2004.11.012

538 Gooseff, M. N., D. M. McKnight, R. L. Runkel, and J. H. Duff. 2004. Denitrification and
539 hydrologic transient storage in a glacial meltwater stream, McMurdo Dry Valleys,
540 Antarctica. Limnol. Oceanogr. **49**: 1884–1895. doi:10.4319/lo.2004.49.5.1884
541 Gootman, K. S., R. G. Pinzón, J. L. A. Knapp, V. Garayburu-Caruso, and J. Cable. 2020.
542 Spatiotemporal Variability in Transport and Reactive Processes Across a First - to Fifth -
543 Order Fluvial Network Water Resources Research. 1–18. doi:10.1029/2019WR026303
544 Hall, R. J. O., E. S. Bernhardt, and G. E. Likens. 2002. Relating nutrient uptake with transient
545 storage in forested mountain streams. Limnol. Oceanogr. **47**: 255–265.
546 doi:10.4319/lo.2002.47.1.0255
547 Hall, R. O., J. L. Tank, D. J. Sobota, and others. 2009. Nitrate removal in stream ecosystems
548 measured by 15N addition experiments: Total uptake. Limnol. Oceanogr. **54**: 653–665.
549 doi:10.4319/lo.2009.54.3.0653
550 Harvey, J. W., J. K. Böhlke, M. A. Voytek, D. Scott, and C. R. Tobias. 2013. Hyporheic zone
551 denitrification: Controls on effective reaction depth and contribution to whole-stream
552 mass balance. Water Resour. Res. **49**: 6298–6316. doi:10.1002/wrcr.20492
553 Harvey, J. W., J. E. Saiers, and J. T. Newlin. 2005. Solute transport and storage mechanisms in
554 wetlands of the Everglades, south Florida. Water Resour. Res. **41**.
555 doi:10.1029/2004WR003507
556 Hill, B. H., C. M. Elonen, L. R. Seifert, A. A. May, and E. Tarquinio. 2012. Microbial enzyme
557 stoichiometry and nutrient limitation in US streams and rivers. Ecol. Indic. **18**: 540–551.
558 doi:10.1016/j.ecolind.2012.01.007
559 Jackson, T. R., S. V. Apte, R. Haggerty, and R. Budwig. 2015. Flow structure and mean
560 residence times of lateral cavities in open channel flows: influence of bed roughness and
561 shape. Environ. Fluid Mech. **15**: 1069–1100. doi:10.1007/s10652-015-9407-2
562 Jackson, T. R., R. Haggerty, S. V. Apte, A. Coleman, and K. J. Drost. 2012. Defining and
563 measuring the mean residence time of lateral surface transient storage zones in small
564 streams. Water Resour. Res. **48**. doi:10.1029/2012WR012096
565 Jackson, T. R., R. Haggerty, S. V. Apte, and B. L. O'Connor. 2013. A mean residence time
566 relationship for lateral cavities in gravel-bed rivers and streams: Incorporating streambed
567 roughness and cavity shape. Water Resour. Res. **49**: 3642–3650. doi:10.1002/wrcr.20272
568 Kasahara, T., and S. M. Wondzell. 2003. Geomorphic controls on hyporheic exchange flow in
569 mountain streams. Water Resour. Res. **39**: SBH 3-1-SBH 3-14.
570 doi:10.1029/2002wr001386
571 Katz, S. B., C. Segura, and D. R. Warren. 2018. The influence of channel bed disturbance on
572 benthic Chlorophyll a: A high resolution perspective. Geomorphology **305**: 141–153.
573 doi:10.1016/j.geomorph.2017.11.010
574 Kelleher, C., T. Wagener, B. McGlynn, A. S. Ward, M. N. Gooseff, and R. A. Payn. 2013.
575 Identifiability of transient storage model parameters along a mountain stream. Water
576 Resour. Res. **49**: 5290–5306. doi:10.1002/wrcr.20413
577 Kiel, B. A., and M. Bayani Cardenas. 2014. Lateral hyporheic exchange throughout the
578 Mississippi River network. Nat. Geosci. **7**: 413–417. doi:10.1038/ngeo2157
579 Knapp, J. L. A., R. González-Pinzón, J. D. Drummond, L. G. Larsen, O. A. Cirpka, and J. W.
580 Harvey. 2017. Tracer-based characterization of hyporheic exchange and benthic biolayers
581 in streams. Water Resour. Res. **53**: 1575–1594. doi:10.1002/2016WR019393

582 Knapp, J. L. A., R. González-Pinzón, and R. Haggerty. 2018. The Resazurin-Resorufin System:
583 Insights From a Decade of "Smart" Tracer Development for Hydrologic Applications.
584 Water Resour. Res. **54**: 6877–6889. doi:10.1029/2018WR023103
585 Knapp, J. L. A., and C. Kelleher. 2020. A Perspective on the Future of Transient Storage
586 Modeling: Let's Stop Chasing Our Tails. Water Resour. Res. **56**: e2019WR026257.
587 doi:10.1029/2019WR026257
588 Krause, S., J. Lewandowski, N. B. Grimm, and others. 2017. Ecohydrological interfaces as hot
589 spots of ecosystem processes: ECOHYDROLOGICAL INTERFACES AS HOT SPOTS.
590 Water Resour. Res. **53**: 6359–6376. doi:10.1002/2016WR019516
591 Lane, C. S., D. R. Lyon, and S. E. Ziegler. 2012. Cycling of two carbon substrates of contrasting
592 lability by heterotrophic biofilms across a nutrient gradient of headwater streams. Aquat.
593 Sci. **75**: 235–250. doi:10.1007/s00027-012-0269-0
594 Lautz, L. K., and D. I. Siegel. 2007. The effect of transient storage on nitrate uptake lengths in
595 streams: an inter-site comparison. Hydrol. Process. **21**: 3533–3548. doi:10.1002/hyp.6569
596 Li, L., P. L. Sullivan, P. Benettin, and others. 2021. Toward catchment hydro-biogeochemical
597 theories. Wiley Interdiscip. Rev. Water **8**: 1–31. doi:10.1002/wat2.1495
598 Li, Z., Z. Zeng, D. Tian, and others. 2020. The stoichiometry of soil microbial biomass
599 determines metabolic quotient of nitrogen mineralization. Environ. Res. Lett. **15**: 034005.
600 doi:10.1088/1748-9326/ab6a26
601 Liu, S., T. Maavara, C. B. Brinkerhoff, and P. A. Raymond. 2022. Global Controls on DOC
602 Reaction Versus Export in Watersheds: A Damköhler Number Analysis. Glob.
603 Biogeochem. Cycles **36**: e2021GB007278. doi:10.1029/2021GB007278
604 Logue, J. B., C. A. Stedmon, A. M. Kellerman, N. J. Nielsen, A. F. Andersson, H. Laudon, E. S.
605 Lindström, and E. S. Kritzberg. 2016. Experimental insights into the importance of
606 aquatic bacterial community composition to the degradation of dissolved organic matter.
607 ISME J. **10**: 533–545. doi:10.1038/ismej.2015.131
608 Martí, E., N. B. Grimm, and S. G. Fisher. 1997. Pre- and Post-Flood Retention Efficiency of
609 Nitrogen in a Sonoran Desert Stream. J. North Am. Benthol. Soc. **16**: 805–819.
610 doi:10.2307/1468173
611 Mulholland, P. J., and W. R. Hill. 1997. Seasonal patterns in streamwater nutrient and dissolved
612 organic carbon concentrations: Separating catchment flow path and in-stream effects.
613 Water Resour. Res. **33**: 1297–1306. doi:10.1029/97wr00490
614 Natural Resources Conservation Service. Web Soil Survey. U. S. Dep. Agric.
615 Navel, S., F. Mermillod-Blondin, B. Montuelle, E. Chauvet, L. Simon, and P. Marmonier. 2011.
616 Water-Sediment Exchanges Control Microbial Processes Associated with Leaf Litter
617 Degradation in the Hyporheic Zone: A Microcosm Study. Microb. Ecol. **61**: 968–979.
618 doi:10.1007/s00248-010-9774-7
619 Niyogi, D. K., K. S. Simon, and C. R. Townsend. 2004. Land use and stream ecosystem
620 functioning: nutrient uptake in streams that contrast in agricultural development. Arch.
621 Für Hydrobiol. **160**: 471–486. doi:10.1127/0003-9136/2004/0160-0471
622 Ocampo, C., Oldham, C., and Sivapalan, M. 2020. Nitrate attenuation in agricultural catchments:
623 Shifting balances between transport and reaction - Ocampo - 2006 - Water Resources
624 Research - Wiley Online Library.
625 Oldham, C. E., D. E. Farrow, and S. Peiffer. 2013. A generalized Damköhler number for
626 classifying material processing in hydrological systems. Hydrol. Earth Syst. Sci. **17**:
627 1133–1148. doi:10.5194/hess-17-1133-2013

628 Perkins, D. M., G. Yvon-Durocher, B. O. L. Demars, J. Reiss, D. E. Pichler, N. Friberg, M.
629 Trimmer, and G. Woodward. 2012. Consistent temperature dependence of respiration
630 across ecosystems contrasting in thermal history. Glob. Change Biol. **18**: 1300–1311.
631 doi:10.1111/j.1365-2486.2011.02597.x
632 Pinay, G., S. Peiffer, J.-R. De Dreuzy, and others. 2015. Upscaling Nitrogen Removal Capacity
633 from Local Hotspots to Low Stream Orders' Drainage Basins. Ecosystems **18**: 1101–
634 1120. doi:10.1007/s10021-015-9878-5
635 Ries III, K. G., J. K. Newson, M. J. Smith, and others. 2017. StreamStats, version 4.
636 Ryan, R. J., A. I. Packman, and S. S. Kilham. 2007. Relating phosphorus uptake to changes in
637 transient storage and streambed sediment characteristics in headwater tributaries of
638 Valley Creek, an urbanizing watershed. J. Hydrol. **336**: 444–457.
639 doi:10.1016/j.jhydrol.2007.01.021
640 Schmid, B. H., I. Innocenti, and U. Sanfilippo. 2010. Characterizing solute transport with
641 transient storage across a range of flow rates: The evidence of repeated tracer
642 experiments in Austrian and Italian streams. Adv. Water Resour. **33**: 1340–1346.
643 doi:10.1016/j.advwatres.2010.06.001
644 Sheibley, R. W., J. H. Duff, and A. J. Tesoriero. 2014. Low Transient Storage and Uptake
645 Efficiencies in Seven Agricultural Streams: Implications for Nutrient Demand. J.
646 Environ. Qual. **43**: 1980–1990. doi:10.2134/jeq2014.01.0034
647 Smith, R. A., R. B. Alexander, and G. E. Schwarz. 2003. Natural background concentrations of
648 nutrients in streams and rivers of the conterminous United States. Environ. Sci. Technol.
649 **37**: 3039–3047. doi:10.1021/es020663b
650 Thomas, S. A., H. Maurice Valett, J. R. Webster, and P. J. Mulholland. 2003. A regression
651 approach to estimating reactive solute uptake in advective and transient storage zones of
652 stream ecosystems. Adv. Water Resour. **26**: 965–976. doi:10.1016/S0309-
653 1708(03)00083-6
654 Tromboni, F., S. A. Thomas, B. Gücker, and others. 2018. Nutrient Limitation and the
655 Stoichiometry of Nutrient Uptake in a Tropical Rain Forest Stream. J. Geophys. Res.
656 Biogeosciences **123**: 2154–2167. doi:10.1029/2018JG004538
657 Valett, H. M., J. A. Morrice, C. N. Dahm, and M. E. Campana. 1996. Parent lithology, surface-
658 groundwater exchange, and nitrate retention in headwater streams. Limnol. Oceanogr. **41**:
659 333–345. doi:10.4319/lo.1996.41.2.0333
660 Vrugt, J. A., C. J. F. Ter Braak, C. G. H. Diks, B. A. Robinson, J. M. Hyman, and D. Higdon.
661 2009. Accelerating Markov Chain Monte Carlo Simulation by Differential Evolution
662 with Self-Adaptive Randomized Subspace Sampling. Int. J. Nonlinear Sci. Numer. Simul.
663 **10**. doi:10.1515/IJNSNS.2009.10.3.273
664 Wagner, K., M. M. Bengtsson, R. H. Findlay, T. J. Battin, and A. J. Ulseth. 2017. High light
665 intensity mediates a shift from allochthonous to autochthonous carbon use in
666 phototrophic stream biofilms. J. Geophys. Res. Biogeosciences **122**: 1806–1820.
667 doi:10.1002/2016JG003727
668 Ward, A. S., and A. I. Packman. 2019. Advancing our predictive understanding of river corridor
669 exchange. Wiley Interdiscip. Rev. Water **6**: e1327. doi:10.1002/wat2.1327
670 Ward, A. S., R. A. Payn, M. N. Gooseff, B. L. McGlynn, K. E. Bencala, C. A. Kelleher, S. M.
671 Wondzell, and T. Wagener. 2013. Variations in surface water-ground water interactions
672 along a headwater mountain stream: Comparisons between transient storage and water
673 balance analyses. Water Resour. Res. **49**: 3359–3374. doi:10.1002/wrcr.20148

Webster, J. R., P. J. Mulholland, J. L. Tank, and others. 2003. Factors affecting ammonium uptake in streams - an inter-biome perspective. Freshw. Biol. **48**: 1329–1352. doi:10.1046/j.1365-2427.2003.01094.x

Wen, H., and L. Li. 2018. An upscaled rate law for mineral dissolution in heterogeneous media: The role of time and length scales. Geochim. Cosmochim. Acta **235**: 1–20. doi:10.1016/j.gca.2018.04.024

Wilhelm, L., K. Besemer, L. Fragner, H. Peter, W. Weckwerth, and T. J. Battin. 2015. Altitudinal patterns of diversity and functional traits of metabolically active microorganisms in stream biofilms. ISME J. **9**: 2454–2464. doi:10.1038/ismej.2015.56

Wondzell, S. M. 2006. Effect of morphology and discharge on hyporheic exchange flows in two small streams in the Cascade Mountains of Oregon, USA. Hydrol. Process. **20**: 267–287. doi:10.1002/hyp.5902

Zarnetske, J. P., M. N. Gooseff, T. R. Brosten, J. H. Bradford, J. P. McNamara, and W. B. Bowden. 2007. Transient storage as a function of geomorphology, discharge, and permafrost active layer conditions in Arctic tundra streams. Water Resour. Res. **43**: 7410. doi:10.1029/2005WR004816

Zarnetske, J. P., R. Haggerty, S. M. Wondzell, V. A. Bokil, and R. González-Pinzón. 2012. Coupled transport and reaction kinetics control the nitrate source-sink function of hyporheic zones. Water Resour. Res. **48**. doi:10.1029/2012wr011894